nature nanotechnology

LETTERS

PUBLISHED ONLINE: 8 JULY 2012 | DOI: 10.1038/NNANO.2012.109

Characterization of the motion of membrane proteins using high-speed atomic force microscopy

Ignacio Casuso[1], Jonathan Khao[2], Mohamed Chami[3], Perrine Paul-Gilloteaux[4], Mohamed Husain[1], Jean-Pierre Duneau[2], Henning Stahlberg[3], James N. Sturgis[2] and Simon Scheuring[1]*

For cells to function properly[1], membrane proteins must be able to diffuse within biological membranes. The functions of these membrane proteins depend on their position and also on protein–protein and protein–lipid interactions[2]. However, so far, it has not been possible to study simultaneously the structure and dynamics of biological membranes. Here, we show that the motion of unlabelled membrane proteins can be characterized using high-speed atomic force microscopy[3]. We find that the molecules of outer membrane protein F (OmpF) are widely distributed in the membrane as a result of diffusion-limited aggregation, and while the overall protein motion scales roughly with the local density of proteins in the membrane, individual protein molecules can also diffuse freely or become trapped by protein–protein interactions. Using these measurements, and the results of molecular dynamics simulations, we determine an interaction potential map and an interaction pathway for a membrane protein, which should provide new insights into the connection between the structures of individual proteins and the structures and dynamics of supramolecular membranes.

Membrane protein diffusion plays an important role in cellular processes, ensuring the proper distribution of molecules as well as bringing them into transient contact with functional partners[4]. Outer membrane protein F (OmpF) is the major porin in the outer membrane of *Escherichia coli*, where it forms trimeric channels for the passage of water, ions, sugars, polar nutrients and waste up to 700 Da in weight[5,6]. Diffusion in the membrane is an important factor in the function of OmpF as it has to be widely distributed on the cell surface for phage recognition[7] to occur, and also has to form a transient translocon with vitamin B_{12} receptor BtuB for colicin import[8,9].

Here, we use high-speed atomic force microscopy (HS-AFM) to study the diffusion, dynamics and organization of unlabelled OmpF in near-native conditions. OmpF co-purified with the natural outer membrane component lipopolysaccharide (LPS) (Supplementary Fig. S1) was reconstituted into *E. coli* lipids at a realistic surface density of ~50% (1×10^5 molecules per cell with a surface area[5] of ~10 μm^2) and imaged in physiological buffer at ambient temperature and pressure. Under these experimental conditions we were able to acquire movies that show with unprecedented resolution the translational and rotational dynamics of these unlabelled membrane proteins in a membrane environment (Fig. 1a, Supplementary Movie S1). Detailed analysis allowed us to gain novel insights into the factors governing protein organization and dynamics, in particular the conformations, energetics and pathways of membrane mediated interaction between membrane proteins. We used cross-correlation-based algorithms[10] to analyse membrane organization and the motion of individual molecules in each frame (750 Å)^2. The particle location and orientation were defined with Ångström precision and with a time resolution of 477 ms over a period of minutes (Fig. 1b,c; technical details can be found in the Materials and Methods section in the Supplementary Information).

We first used fractal analysis to provide a quantitative assessment of the complexity and order in the two-dimensional arrangement of OmpF molecules in the membrane[11]. The overall molecular distribution of the OmpF in the membrane showed a highly intricate geometry with high fractal dimension $D \approx 1.73 \pm 0.01$ (Supplementary Fig. S2), which is characteristic of diffusion-limited aggregation[12]. Such a fractality optimizes the membrane distribution of OmpF to provide a wide variety of local environments and interaction possibilities for individual molecules, which is probably important for the dynamic formation of translocon complexes[13]. For comparison, a simulation of OmpF arranged in a two-dimensional array had a fractal dimension of $D \approx 1.05 \pm 0.02$, so the OmpF in our experiments expose about twice as much molecular surface as molecules in a regular array (Supplementary Fig. S2).

Different local environments strongly affect the dynamics of individual membrane proteins. For example, crowding has previously been identified as a possible source of limited diffusion[14] but was exclusively examined with modelling[15]. With HS-AFM, a technique that allows for the explicit observation of the environment of a moving protein, we can now experimentally assess the effect of crowding for the first time.

To analyse this crowding effect we traced the molecular movements and measured the available area for each molecule using Voronoi tessellation[16] of the surface (Fig. 1d). The borders between Voronoi cells are equidistant from the two closest molecules. A clear trend correlating increased molecular motion with increased available membrane area can be established. Voronoi cell areas show a distribution ranging from ~7,000 Å^2 to ~20,000 Å^2, peaking at ~12,000 Å^2 (for comparison the membrane area occupied by a projected X-ray structure trimer[17] is ~4,700 Å^2, and trimers in two-dimensional crystals[18] occupy ~5,700 Å^2) (Supplementary Fig. S3). The histogram of the areas of the Voronoi cells shows that the majority of molecules are confined into a small membrane space, with a few molecules disposed in a free membrane area much larger than the average area, these being the molecules that actually diffuse. Interestingly, some molecules that are located in large Voronoi cells do not display motion (Fig. 1d, red star). These molecules appear to participate in characteristic assemblies that are stable over time. These

[1]U1006 INSERM, Aix-Marseille Université, Parc Scientifique et Technologique de Luminy, 163 avenue de Luminy, 13009 Marseille, France, [2]UPR-9027 LISM, CNRS-Aix-Marseille University, Marseille, 13402, France, [3]Center for Cellular Imaging and NanoAnalytics (C-CINA), Biozentrum, University Basel, Mattenstrasse 26, WRO-1058, CH-4058 Basel, Switzerland, [4]Cell and Tissue Imaging Facility (PICT-IBiSA), UMR144 CNRS-Institut Curie, 26 rue d'Ulm, Paris, F-75248 France. *e-mail: simon.scheuring@inserm.fr

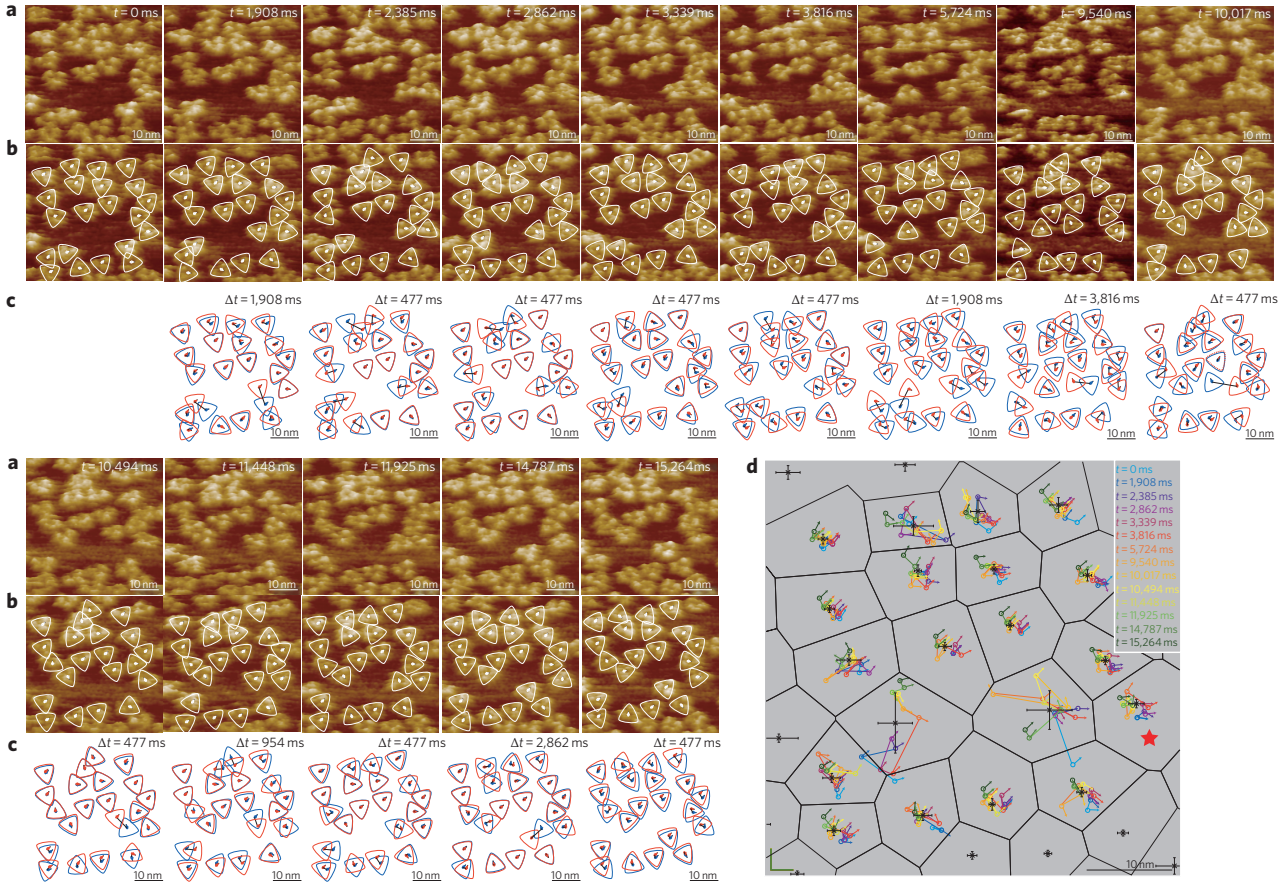

Figure 1 | HS-AFM movie frames showing the motion of OmpF trimers in the membrane. Full movie length, 115,434 ms; frame rate, 477 ms; full image size, 750 Å; full frame size, 300 pixels (Supplementary Movie S1). **a**, Individual HS-AFM frames. The individual subunits of the OmpF trimers are resolved. **b**, As in **a**, but with an overlaid outline of OmpF trimer localization and orientation. **c**, Molecular positions in the current frame (red outlines) compared with those of the previous frame (blue outlines) with displacement shown as black lines. **d**, Molecular displacement traces and orientations (arrows) as analysed in **c**. Note that the angular orientation depicts one subunit of the trimeric porin OmpF. Black crosses and bars display the average and standard deviation of the position of the molecules. The network overlay presents the Voronoi tessellation defining the free membrane area of each molecule.

particular protein–protein interactions often show specific symmetry relations with neighbouring molecules. They appear to assemble most frequently by intercalating their subunit grooves or by interacting with their subunit apex (Supplementary Fig. S4, Supplementary Movies S2 and S3). These associations are discussed in detail in the following.

We also report the diversity of molecular motion within the membrane by calculating a membrane heat-map[19], which displays the average velocity of OmpF motion at each location over time (Supplementary Fig. S5). The heat-map shows areas of high velocity and areas where molecules are essentially immobile throughout the movie acquisition as a result of local and neighbourhood-dependent molecular motion (Supplementary Movie S4). In conclusion, the dynamics of the molecules seem to be dominated by crowding and specific interactions between neighbours.

The variation in the molecular motion, with some molecules being essentially immobile and trapped but others diffusing temporally (as can be seen in the HS-AFM movie; Fig. 1, Supplementary Movie S1), precludes the calculation of an effective diffusion constant. An example of a track of an essentially immobile molecule reveals only minor displacements (Fig. 2a, blue); it rattles around a fixed position (Fig. 2b, blue), and the calculated mean square displacement (MSD) as a function of the lag time indicates corralled sub-diffusive behaviour[20] (Fig. 2c, blue). In contrast, some molecules move more rapidly, with a maximum measured velocity of $\sim$25 nm s^{-1} (Fig. 2a, red) within a Voronoi cell of area $\sim$20,000 Å^2 (Fig. 2b, red). Such molecules diffuse freely over a long timescale, as shown by the slope of $\sim$1.1 in the log(MSD) versus log(Δt) plot of Fig. 2c (red).

The dynamics of the molecules are not biased by the HS-AFM tip interaction, as no directional correlation with the fast scan axis is observed (Supplementary Fig. S6). Furthermore, under the imaging conditions used, we estimate the applied force to be too low to affect molecular movement ($\sim$50 pN; refs 21,22), and the tip interacts with the sample only $\sim$1.6 times on each pixel over $\sim$160 ns. Additionally, we ruled out scan direction bias by increasing the HS-AFM imaging speed to 204 ms per frame, and found similar molecule dynamics (Supplementary Fig. S6 and Movie S5). Spector and colleagues[13] reported that fluorophore-antibody-labelled OmpF in cells diffused much more quickly within an area with a diameter of 100 nm than reported here. These discrepancies can originate from variations in membrane crowding, different timescales ($<$250 ms), different experimental procedures and potential frictional coupling with the support through the thin lubrication layer.

Early electron microscopy studies have indicated a high density of porin packing in the outer membrane, which is likely to result in significantly restricted protein movement[5,23]. In the crowded membrane, HS-AFM provides evidence that the displacement of one molecule can induce a chain motion, allowing movement of another molecule (Supplementary Fig. S7 and Movies S6 and S7).

As well as the analysis of the lateral motion of the OmpF, the sub-molecular resolution of our topographs allows the angular

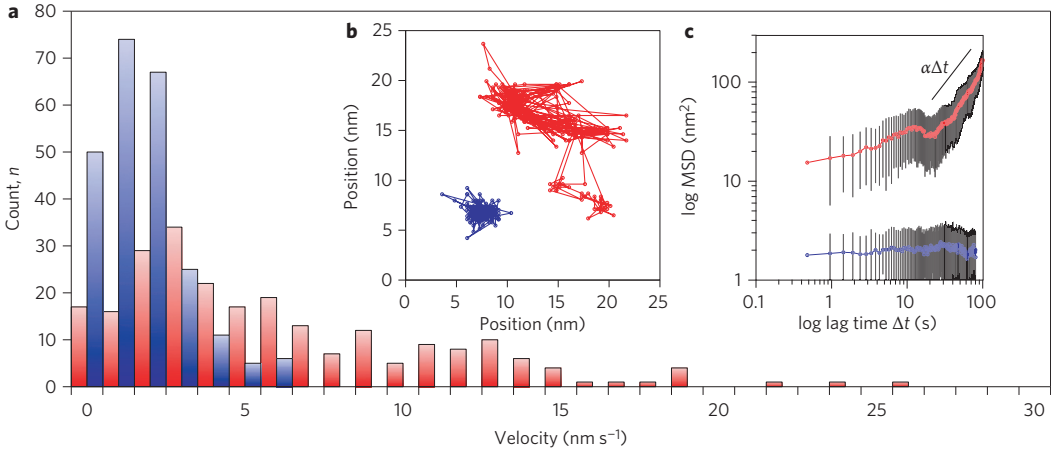

Figure 2 | Diffusion analysis of OmpF. a, Histogram of the displacement velocity of the molecules: blue, representative immobile molecule participating in a stable association; red, representative diffusing molecule. **b**,**c**, Diffusion traces (**b**) and MSD as a function of lag time (**c**) of the two molecules. The derived exponent values (fit±s.d.) are $\alpha = 0.1 \pm 0.1$ and $\alpha = 1.1 \pm 0.2$ for the immobile and diffusing molecule, respectively.

orientation of each molecule to be determined. In an overall analysis of the data (recorded at a frame rate of 477 ms), the rotation coefficient cannot be determined. About 80% of the molecules are relatively stable and only rattle slightly about their preferred orientation, while the remaining ~20% of free molecules randomize their orientation between consecutive frames (Supplementary Fig. S8A). Again, single molecules display different behaviours, depending on their molecular interactions (Supplementary Fig. S8B and Movie S8). As expected from the ensemble analysis, plotting rotation as a function of molecular displacement suggests only a weak tendency for scaled lateral and rotational movement; molecules involved in short-distance protein–protein interactions barely rotate, in contrast to free molecules (Supplementary Fig. S8C). Rotation and diffusion in a viscous bilayer have the same physical basis, so molecules that move 10 nm in 477 ms (frame rate) can rotate through more than 120° given that the distance between subunits within a trimer is ~3 nm. A much higher scan rate is therefore needed to assess rotational dynamics.

To better understand our results and provide molecular insights about OmpF interactions, we performed molecular dynamics simulations (MDS) to examine the energetics and dynamics of OmpF trimers in a hydrated phospholipid bilayer. In these simulations we studied the dissociation of interacting proteins. The steered MDS suggests a specific reaction pathway for the association and dissociation of OmpF that involves coordinated separation and rotation as it passes through several configurations (Fig. 3a, Supplementary Movie S9). The simulation suggests that this pathway is determined by solvation–desolvation by lipids of the membrane-embedded protein surfaces. At short centre-to-centre distances, protein–protein contacts are preserved to avoid the creation of interstitial voids that would need to be filled with lipid molecules. In the simulation, as the separation distance increases, the two OmpF surfaces in 'base-to-base' contact (Fig. 3a, label 'a') first undergo a shear and rotation motion that gradually replaces protein–protein contacts with protein–lipid interactions. This motion results in a 'base-to-tip' assembly (Fig. 3a, label 'b'). In a second step, a hinge motion takes place, leading to a 'tip-to-tip' configuration (Fig. 3a, label 'c'). In this arrangement the protein–protein contact is minimized and the energetic cost for separation is as low as possible.

To estimate the energetics of the interaction between two OmpF trimers we used umbrella sampling to integrate the interaction potential along the dissociation pathway. In this potential energy map, 'base-to-base' and 'tip-to-tip' associations both correspond to stable configurations in potential wells (Fig. 3a). Despite the constraining potential and the length of the simulation, some high-energy transition states might be poorly sampled in the interaction energy profile. These are configurations in which lipids between the two OmpF trimers are reorganized. Thus, although the examined dissociation pathway, the observed structures and the qualitative aspects of the energetic landscape are solid, the quantitative aspects of the energy profile should be interpreted with caution (Fig. 3a). It is noteworthy that the shape of the energy landscape calculated from the MDS is in agreement with that calculated from pair correlation function analysis of the molecular arrangements in the images, notably with a deep well corresponding to the 'base-to-base' arrangement at 7 nm (data not shown).

Despite the fact that the HS-AFM observations of reversible OmpF associations are very different in terms of timescale compared to MDS, the same conformations are found experimentally. Two OmpF trimers sample the same series of associations before dissociating from a 'tip-to-tip' arrangement and reorganizing with other partners (Fig. 3b). The HS-AFM imaging depicts the detailed molecular position and rotation of ~17,000 molecules (~70 in each of the 239 frames), representing a large dataset of conformations to calculate the probability density map of molecular arrangements (Fig. 3c, Supplementary Movie S10). This density map shows that the most frequent associations (depicted by triangle-pair symbols in Fig. 3c) are linked by high-density connections, suggesting that a low-energy pathway for structural interconversion exists, in agreement with the steered coarse-grained MDS (Fig. 3a).

In the experimental map (Fig. 3c), the most occupied basins correspond to the 'base-to-base', 'base-to-tip' and 'tip-to-tip' configurations, in agreement with those observed along the dissociation pathway (Fig. 3b) and in local minima of the computed free energy profile (Fig. 3a). The structural specificities of these configurations stem from the atomic properties of the OmpF surfaces that are reflected in the experimental data and retained in coarse-grained molecular models. It must be noted that the shortest-distance conformation—'base-to-base'—engages the largest possible interfaces between inter-subunit grooves of the molecules, and is thus particularly stable. Furthermore, the simulation predicts a repulsive regime at a centre-to-centre separation distance larger than 9 nm (Fig. 3a, labels 'd' and 'e'), which is probably lipid-mediated due to protein membrane perturbation[24]. This repulsion may be reflected in the HS-AFM measurements by molecules undergoing chain-like movements between neighbours (Supplementary Fig. S7).

It has been rationalized that membrane protein diffusion is influenced by crowding[25], protein size[26] or by various more

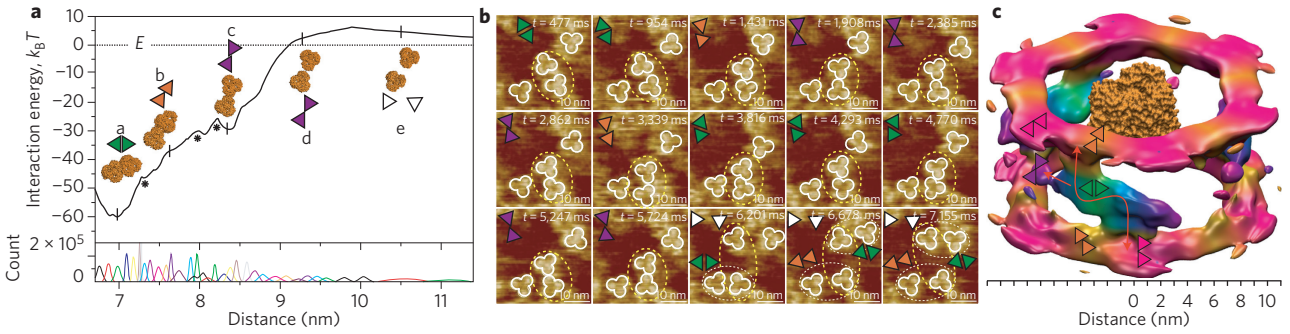

Figure 3 | MDS and experimental evaluation of OmpF–OmpF interaction pathway and potential. a, Potential energy landscape from coarse-grained MDS. Top: interaction energy between two molecules in the membrane as a function of distance with a shortest contact association well at a centre-to-centre distance of 7 nm and a repulsive regime at separations further than 9 nm. The trajectory traverses 'base-to-base', 'tip-to-base' and 'tip-to-tip' configurations at distances of 7.0 nm, 7.5 nm and 8.5 nm, respectively, until loss of molecular contact at 9.5 nm. Asterisks indicate high-energy intermediate configurations that are probably under-sampled. Bottom: umbrella sampling histograms used to construct the potential. **b**, The separation of two OmpF proteins implies molecular shear and rotational movements. The observed transition comprises all of the major interaction states that are low-energy states in the coarse-grained MDS shown in **a**. The two molecules are initially in a 'base-to-base' association (477 ms), then, via a rotational rearrangement, they translate into a 'tip-to-tip' configuration (1,908 ms); further rotation brings them back into a 'base-to-tip' association (3,339 ms), before engaging again in a 'tip-to-tip' association (5,247 ms, 5,724 ms) then separation (6,201 ms). The two central molecules are identified within yellow dashed lines, and triangle symbols in the top left corner represent their interaction state (white triangles represent loss of contact as in **a**). Both molecules engage in relationships with neighbouring molecules (6,678 ms, 7,155 ms) (Supplementary Movie S6). **c**, Experimental interaction probability map: a multidimensional representation, where the radial distance is the centre-to-centre distance (*r*, nm) between two molecules, the polar coordinate describes the localization of the neighbouring molecule with respect to the central molecule, the colour coding on the vertical dimension represents the relative orientation between the two molecules, with pairs of triangle symbols (as in **a** and **b**) on the densities indicating the respective orientation of trimers occurring with high probability. The three-dimensional density surface is set at fivefold enrichment relative to the mean probability.

complicated mechanisms in eukaryotes[27]. Our data show that crowding and/or size are important, but not sufficient to explain the varying diffusion behaviour. Indeed specific protein–protein interactions play a crucial role. In the outer *E. coli* membrane, all membrane proteins experience on average the same crowding. Furthermore, the outer membrane porins OmpF[17] and trimeric maltoprotein LamB[28] are structurally very similar trimers. Previously, it has been reported that the diffusion properties of OmpF and LamB differ by up to two orders of magnitude[13]. This can be rationalized neither by the overall crowding nor by their size. Here, we show that individual molecules can show diffusive behaviour and engage in immobile stable assemblies with preferential protein–protein contacts. The formation of specific associations increases when a protein is abundant, as the probability of meeting in two dimensions scales with the number of molecules[29]. Hence, crowding is essential but must be considered for each protein species. Indeed OmpF is the most abundant outer membrane protein[5] and will therefore encounter most interaction partners. Consequently, due to specific interactions, proteins that form stable large ensembles with OmpF will feature slowed diffusion (logarithmically[26] or proportionally[30]). Furthermore, such ensembles are more sensitive to being hindered in a crowded environment. Future experiments will address the interaction behaviour of less abundant protein species and the interaction between different types of outer membrane proteins.

In summary, we have analysed the influence of membrane crowding on the motion of individual molecules within a membrane and have presented a first interaction potential map and interaction pathway for a membrane protein. We have also discussed the parameters that can explain anomalous diffusion and have demonstrated the propensity of membrane proteins to participate in functional ensembles. It is clear that the membrane protein sequences have not only evolved at the 'molecular core' so as to perfect their biological function (for example, transport), but have also evolved in terms of their membrane exposed surfaces to accomplish interaction.

Methods

The bacterial outer membrane protein OmpF associated with LPS was produced in *E. coli* and purified in 10 mg ml^{-1} of octyl-polyoxyethylene. The complexes were mixed with *E. coli* lipids at a lipid-to-protein ratio of 0.5. Reconstitution occurred via detergent removal by using dialysis against 20 mM HEPES–NaOH (pH 7) buffer supplemented with 100 mM NaCl and 10 mM $MgCl_2$.

HS-AFM observations were performed in oscillating mode using optimized high-resolution imaging parameters. Short cantilevers designed for HS-AFM with a length of ~6 μm, a spring constant of 0.1–0.2 N m^{-1}, a resonance frequency of 600 kHz and a quality factor of ~2 in solution were used, bearing an electron beam deposition tip at the end of the cantilever. The sensitivity of the AFM system to probe deflection was 0.1 V nm^{-1}. The free amplitude was ~10 Å and the imaging amplitude setpoint was set to ~90% of the free amplitude. Under such conditions, the force applied by the HS-AFM tip on the sample was estimated to be <100 pN.

Received 3 April 2012; accepted 4 June 2012;
published online 8 July 2012

References

1. Engelman, D. M. Membranes are more mosaic than fluid. *Nature* **438,** 578–580 (2005).
2. Phillips, R., Ursell, T., Wiggins, P. & Sens, P. Emerging roles for lipids in shaping membrane–protein function. *Nature* **459,** 379–385 (2009).
3. Ando, T. *et al.* A high-speed atomic force microscope for studying biological macromolecules. *Proc. Natl Acad. Sci. USA* **98,** 12468–12472 (2001).
4. Schmidt, T., Schütz, G. J., Baumgartner, W., Gruber, H. J. & Schindler, H. Imaging of single molecule diffusion. *Proc. Natl Acad. Sci. USA* **93,** 2926–2929 (1996).
5. Rosenbusch, P. Characterization of the major envelope protein from *Escherichia coli*. *J. Biol. Chem.* **249,** 8019–8029 (1974).
6. Engel, A., Massalski, A., Schindler, H., Dorset, D. L. & Rosenbusch, J. P. Porin channel triplets merge into single outlets in *Escherichia coli* outer membranes. *Nature* **317,** 643–645 (1985).
7. Foulds, J. & Chai, T. J. New major outer membrane proteins found in an *Escherichia coli* tolF mutant resistant to bacteriophage TuIb. *J. Bacteriol.* **133,** 1478–1483 (1978).
8. Housden, N. G., Loftus, S. R., Moore, G. R., James, R. & Kleanthous, C. Cell entry mechanism of enzymatic bacterial colicins: porin recruitment and the thermodynamics of receptor binding. *Proc. Natl Acad. Sci. USA* **102,** 13849–13854 (2005).
9. Yamashita, E., Zhalnina, M. V., Zakharov, S. D., Sharma, O. & Cramer, W. A. Crystal structures of the OmpF porin: function in a colicin translocon. *EMBO J.* **27,** 2171–2180 (2008).

10. Husain, M., Boudier, T., Paul-Gilloteaux, P., Casuso, I. & Scheuring, S. Software for drift compensation, particle tracking and particle analysis of high-speed atomic force microscopy image series. *J. Mol. Recognit.* **25,** 292–298 (2012).
11. Smith, T. G. Jr, Lange, G. D. & Marks, W. B. Fractal methods and results in cellular morphology—dimensions, lacunarity and multifractals. *J. Neurosci. Methods* **69,** 123–136 (1996).
12. Witten, T. A. & Sander, L. M. Diffusion-limited aggregation, a kinetic critical phenomenon. *Phys. Rev. Lett.* **47,** 1400–1403 (1981).
13. Spector, J. *et al*. Mobility of BtuB and OmpF in the *Escherichia coli* outer membrane: implications for dynamic formation of a translocon complex. *Biophys. J.* **99,** 3880–3886 (2010).
14. Kusumi, A., Sako, Y. & Yamamoto, M. Confined lateral diffusion of membrane receptors as studied by single particle tracking (nanovid microscopy). Effects of calcium-induced differentiation in cultured epithelial cells. *Biophys. J.* **65,** 2021–2040 (1993).
15. Mika, J. T. & Poolman, B. Macromolecule diffusion and confinement in prokaryotic cells. *Curr. Opin. Biotechnol.* **22,** 117–126 (2011).
16. Anne, P. Voronoi and Voronoi-related tessellations in studies of protein structure and interaction. *Curr. Opin. Struct. Biol.* **14,** 233–241 (2004).
17. Cowan, S. W. *et al*. Crystal structures explain functional properties of two *E. coli* porins. *Nature* **358,** 727–733 (1992).
18. Hoenger, A., Pages, J. M., Fourel, D. & Engel, A. The orientation of porin OmpF in the outer membrane of *Escherichia coli*. *J. Mol. Biol.* **233,** 400–413 (1993).
19. Serge, A., Bertaux, N., Rigneault, H. & Marguet, D. Dynamic multiple-target tracing to probe spatiotemporal cartography of cell membranes. *Nature Methods* **5,** 687–694 (2008).
20. Marguet, D., Lenne, P. F., Rigneault, H. & He, H. T. Dynamics in the plasma membrane: how to combine fluidity and order. *EMBO J.* **25,** 3446–3457 (2006).
21. García, R. (ed.) in *Amplitude Modulation Atomic Force Microscopy* 77–90 (Wiley, 2010).
22. Uchihashi, T., Iino, R., Ando, T. & Noji, H. High-speed atomic force microscopy reveals rotary catalysis of rotorless F1-ATPase. *Science* **333,** 755–758 (2011).
23. Osborn, M. J. & Wu, H. C. P. Proteins of the outer-membrane of gram-negative bacteria. *Annu. Rev. Microbiol.* **34,** 369–422 (1980).
24. De Meyer, F. J-M., Venturoli, M. & Smit, B. Molecular simulations of lipid-mediated protein–protein interactions. *Biophys. J.* **95,** 1851–1865 (2008).
25. Dix, J. A. & Verkman, A. S. Crowding effects on diffusion in solutions and cells. *Annu. Rev. Biophys.* **37,** 247–263 (2008).
26. Saffman, P. G. & Delbrück, M. Brownian motion in biological membranes. *Proc. Natl Acad. Sci. USA* **72,** 3111–3113 (1975).
27. Kusumi, A. *et al*. Paradigm shift of the plasma membrane concept from the two-dimensional continuum fluid to the partitioned fluid: high-speed single-molecule tracking of membrane molecules. *Annu. Rev. Biophys. Biomol. Struct.* **34,** 351–378 (2005).
28. Schirmer, T., Keller, T. A., Wang, Y. F. & Rosenbusch, J. P. Structural basis for sugar translocation through maltoporin channels at 3.1 Å resolution. *Science* **267,** 512–514 (1995).
29. Melo, E. & Martins, J. Kinetics of bimolecular reactions in model bilayers and biological membranes. A critical review. *Biophys. Chem.* **123,** 77–94 (2006).
30. Gambin, Y. *et al*. Lateral mobility of proteins in liquid membranes revisited. *Proc. Natl Acad. Sci. USA* **103,** 2098–2102 (2006).

Acknowledgements

The authors thank C. Nimigean and F. Rico for critical discussion of the manuscript. The authors also thank P. Abeyrathne for support with the lipopolysaccharide detection. Work in the Scheuring laboratory was supported by the Institut Curie, the Institut National de la Santé et Recherche Médicale (INSERM), the Agence Nationale de la Recherche (ANR) and the City of Paris. Work in the Sturgis laboratory was supported by the Centre National de la Recherche Scientifique (CNRS), the Agence Nationale de la Recherche (ANR), Centre Informatique National de l'Enseignement Superieur (CINES) and Aix-Marseille University. Work in the Stahlberg laboratory was supported by the Swiss National Science Foundation (grant no. 315230_127545, and NCCRs Struct Biol and TransCure) and the Swiss Initiative for Systems Biology (SystemsX.ch).

Author contributions

I.C. and S.S. conceived the experiments. I.C., M.H., M.C. and J.K. performed experiments. I.C., S.S., M.H., P.P-G., J-P.D. and J.N.S. analysed the data. I.C., S.S., J.N.S. and H.S. co-wrote the paper.

Additional information

The authors declare no competing financial interests. Supplementary information accompanies this paper at www.nature.com/naturenanotechnology. Reprints and permission information is available online at http://www.nature.com/reprints. Correspondence and requests for materials should be addressed to S.S.